

Silver nanoparticles inhaled during pregnancy reach and affect the placenta and the foetus

Luisa Campagnolo, Micol Massimiani, Lucia Vecchione, Diletta Piccirilli, Nicola Toschi, Andrea Magrini, Elena Bonanno, Manuel Scimeca, Luca Castagnozzi, Giorgio Buonanno, Luca Stabile, Francesco Cubadda, Federica Aureli, Paul HB Fokkens, Wolfgang G. Kreyling, Flemming R Cassee & Antonio Pietroiusti

To cite this article: Luisa Campagnolo, Micol Massimiani, Lucia Vecchione, Diletta Piccirilli, Nicola Toschi, Andrea Magrini, Elena Bonanno, Manuel Scimeca, Luca Castagnozzi, Giorgio Buonanno, Luca Stabile, Francesco Cubadda, Federica Aureli, Paul HB Fokkens, Wolfgang G. Kreyling, Flemming R Cassee & Antonio Pietroiusti (2017) Silver nanoparticles inhaled during pregnancy reach and affect the placenta and the foetus, *Nanotoxicology*, 11:5, 687-698, DOI: [10.1080/17435390.2017.1343875](https://doi.org/10.1080/17435390.2017.1343875)

To link to this article: <https://doi.org/10.1080/17435390.2017.1343875>



Accepted author version posted online: 16 Jun 2017.
Published online: 07 Jul 2017.



Submit your article to this journal [↗](#)



Article views: 232



View related articles [↗](#)



View Crossmark data [↗](#)










Citing articles: 4 View citing articles [↗](#)

ORIGINAL ARTICLE



Silver nanoparticles inhaled during pregnancy reach and affect the placenta and the foetus

Luisa Campagnolo^a , Micol Massimiani^a, Lucia Vecchione^{a,b} , Diletta Piccirilli^a, Nicola Toschi^a, Andrea Magrini^a, Elena Bonanno^c, Manuel Scimeca^c , Luca Castagnozzi^a, Giorgio Buonanno^{d,e}, Luca Stabile^d , Francesco Cubadda^f , Federica Aureli^f , Paul HB Fokkens^g, Wolfgang G. Kreyling^h , Flemming R Cassee^{g,i} and Antonio Pietroiusti^a

^aDepartment of Biomedicine and Prevention, University of Rome Tor Vergata, Rome, Italy; ^bDepartment of Physics, University of Calabria, Arcavacata di Rende, CS, Italy; ^cDepartment of Experimental Medicine and Surgery, University of Rome Tor Vergata, Rome, Italy; ^dDepartment of Civil and Mechanical Engineering, University of Cassino and Southern Lazio, Cassino, Italy; ^eQueensland University of Technology, Brisbane City, QLD, Australia; ^fDepartment of Food Safety, Nutrition and Veterinary Public Health, Istituto Superiore di Sanità-National Institute of Health, Rome, Italy; ^gNational Institute for Public Health and the Environment, Bilthoven, The Netherlands; ^hHelmholtz Zentrum München, Institute of Epidemiology 2, Neuherberg, Germany; ⁱInstitute for Risk Assessment Studies, Utrecht University, Utrecht, TD, The Netherlands

ABSTRACT

Recently, interest for the potential impact of consumer-relevant engineered nanoparticles on pregnancy has dramatically increased. This study investigates whether inhaled silver nanoparticles (AgNPs) reach and cross mouse placental barrier and induce adverse effects. Apart from their relevance for the growing use in consumer products and biomedical applications, AgNPs are selected since they can be unequivocally identified in tissues. Pregnant mouse females are exposed during the first 15 days of gestation by nose-only inhalation to a freshly produced aerosol of 18–20 nm AgNPs for either 1 or 4 h, at a particle number concentration of 3.80×10^7 part./cm³ and at a mass concentration of 640 µg/m³. AgNPs are identified and quantitated in maternal tissues, placentas and foetuses by transmission electron microscopy coupled with energy-dispersive X-ray spectroscopy and single-particle inductively coupled plasma mass spectrometry. Inhalation of AgNPs results in increased number of resorbed foetuses associated with reduced oestrogen plasma levels, in the 4h/day exposed mothers. Increased expression of pregnancy-relevant inflammatory cytokines is also detected in the placentas of both groups. These results prove that NPs are able to reach and cross the mouse placenta and suggest that precaution should be taken with respect to acute exposure to nanoparticles during pregnancy.

ARTICLE HISTORY

Received 21 February 2017
Revised 19 May 2017
Accepted 14 June 2017

KEYWORDS

Silver nanoparticles; pregnancy; placental barrier; embryo; inhalation exposure

Introduction

Over the last decade, the impact of nanotechnology-based products on public health has been investigated in many experimental settings, both *in vitro* and *in vivo*. Exposure to engineered nanoparticles (NPs) in susceptible populations has been also a matter of concern (Stone et al., 2016). Due to complex metabolic changes and to the higher susceptibility of the developing tissues to environmental hazards, exposure to NPs during pregnancy has become of interest (Hougaard et al., 2015). In mammals, the placenta is the key organ for the maintenance of pregnancy, acting as a semi-permeable barrier for the regulation of nutrient, gas and waste exchange between the mother and the developing foetus. However, the placenta also plays a role in the transfer of xenobiotics to the foetal circulation, which may occur through passive or carrier-mediated transport (Prouillac & Lecoeur, 2010). Several metals have been demonstrated to cross the placental barrier mainly through passive diffusion (Chen et al., 2014; Dencker et al., 1983). Size- and chemistry-dependent barrier capacity of the human placenta to nanoparticles has been demonstrated using an *ex vivo* perfusion model (Myllynen et al., 2008; Wick et al., 2010). However, information on foetal toxicity after maternal exposure to engineered nanomaterials can only be obtained from *in vivo* studies. Some studies have investigated maternal and foetal toxicity of

engineered nanoparticles after intravenous administration. For example, exposure to low dose of single-wall carbon nanotubes (SWCNTs) early in pregnancy, when no placenta is yet formed, induced severe embryo alterations, impaired placental vascularisation and increased oxidative stress in mice (Pietroiusti et al., 2011). More recently, fluorescently labelled SWCNTs have been identified in placentas and in foetal membranes indicating ability of NPs to reach and distribute to these organs (Campagnolo et al., 2013). Specific physicochemical properties were demonstrated important determinants of foetal toxicity, as recently proved for 70 nm non-functionalised silica nanoparticles, whose functionalisation was able to abolish the induced foetal growth restriction after systemic administration close to term (Yamashita et al., 2011). The stage of pregnancy at exposure is also of importance, as reported for intravenously administered gold nanoparticles (Yang et al., 2012). Gold NPs were detected in embryonic tissues when administered up to gestational day (GD) 9.5, after which accumulation was limited to extra-embryonic tissues (Yang et al., 2012). Interestingly, the same study also demonstrated that gold (Au) NPs, although localised in the placenta and the foetus, did not affect development, indicating that the mere presence of NPs in placental and embryonic tissues may not necessarily imply toxicity. Similar results were reported for functionalised silica NPs even at the very high doses

of 1.6 mg intravenously administered to mice (Yamashita et al., 2011). All the mentioned results have been obtained after intravenous administration of NPs, which allows direct correlation between the injected dose and the effect. However, in occupational and environmental settings, transport across primary biological barriers (e.g., the lung epithelium) and subsequent distribution and possible accumulation in the target organs (e.g., the placenta) has to be considered to assess the risk of exposure to airborne NPs during pregnancy. Very few studies have investigated the effect of inhalation exposure to nanoparticles on embryonic development. Nose-only exposure to high dose of cadmium oxide nanoparticles was demonstrated to decrease pregnancy rate and to elevate cadmium content in the placenta and other maternal organs. However, translocation did not occur as no cadmium was detected in fetuses at GD 17.5, although decreased foetal length was observed (Blum et al., 2012). These results were not surprising, since most forms of cadmium have been well documented as reproductive toxicants (Thompson & Bannigan, 2008). More recently, it has been shown that mouse whole body exposure to highly soluble copper NPs did not result in Cu accumulation in the placenta and fetuses, although affected gestational parameters (Adamcaková-Dodd et al., 2015). Altogether, these data indicate that maternal exposure and *in utero* exposure of the foetus are both of concern, and may be responsible for disease processes via a number of direct and indirect mechanisms. Based on the lack of clear information on the ability of moderately soluble NPs to distribute to the placenta and translocate to foetal tissues, and eventually affect directly or indirectly foetal development, we have performed experiments of pulmonary exposure to AgNPs in pregnant mice. Exposure occurred during the first 15 days of gestation, a critical window for foetal development, and biodistribution and foetal-maternal toxicity were evaluated. Silver nanoparticles were chosen for two main reasons: they represent the most widely used type of nanoparticles in consumer products, being present in almost half of nanomaterial-containing goods, including spray deodorants, air conditioners, cosmetics and pesticides (Vance et al., 2015); in addition, nanosilver can be used as model nanoparticles, that can be easily produced, as well as identified and quantitated in tissues using different techniques, allowing distribution studies in foetal tissues to be made.

Methods

Animals

Eight-week-old C57BL/6 female mice were purchased from Charles River (Charles River Laboratories, Calco, Italy), and group housed (10 females per cage) in the Tor Vergata Animal Technology Station under standard conditions, with food and water provided *ad libitum*. All animal procedures were approved by the Ministry of Health (authorisation number 675/2015). Three days prior to mating, soiled bedding from a male's cage was introduced in the female cages to synchronise the oestrous cycles. Some of the females were then mated with males of proven fertility and the presence of a vaginal plug was checked the following morning. The day of the plug was defined as GD 0.5. One group of females was left unmated and was housed in a separate cage until exposure.

Design

Groups of 4–5 pregnant females were exposed by nose-only inhalation to AgNP every day for 1 or 4 h/day (1 h/d and 4 h/d

exposure, respectively), from GD 0.5 to GD 14.5, at a mass concentration of $640 \mu\text{g}/\text{m}^3$. Groups of 4–5 non-pregnant females were exposed in parallel for the same duration. Control pregnant and non-pregnant animals were exposed to filtered air 4 h/day. At the end of each exposure event, animals were allocated back in their cages with water and food, together with their exposure tube for acquaintance. Before starting each new exposure, animals were weighted and signs of distress were monitored, in order to exclude animals displaying discomfort. At the end of the last exposure, pregnant and non-pregnant females were allowed to recover in their cages for 4 h, after which they were sacrificed by cervical dislocation.

Inhalation exposure

The silver nanoparticles were produced by a Palas GFG 1000 (Palas GmbH, Karlsruhe, Germany) spark generator fitted with silver-tipped copper electrodes in inert argon at a flow of 3 L/min. Immediately after generation, the AgNPs were heated up to 600°C in a 30 cm long tube furnace to melt them into spherical particles. To generate the 18 nm nanoparticles in an atmosphere, the output of the generator was immediately diluted with nitrogen and oxygen, to achieve a final concentration of 20% oxygen in the total airflow of 10 L/min. The particle number concentration was controlled by setting the spark frequency to 270 Hz (90% of full scale). The final condition of the aerosol (55% RH, 21°C) was set by adjusting the relative humidity of the mixing gases. Continuous measurements of the test atmosphere were performed during the entire exposure period. In order to precisely measure the parameters of the inhaled aerosol, particle number concentration and size distribution were measured at the breathing zone of the animals. The total particle number concentration was measured over time by a condensation particle counter (CPC 3022, TSI Inc., St. Paul, MN). Particle size distribution was monitored over time by a Scanning Mobility Particle Sizer (SMPS 3936) made up of an Electrostatic Classifier 3080, equipped with a 3081 Long-DMA (TSI Inc., St. Paul, MN) and a 3775 CPC (butanol-based condensation particle counter, TSI Inc., St. Paul, MN). Particle number distributions were measured in the range 6–220 nm considering an aerosol flow rate of 1.5 L/min and a sheath flow rate of 15 L/min. Surface area and volume size distributions were obtained from the particle number distributions considering spherical particles. Temperature and relative humidity were determined by a Vaisala M170 (Vaisala Oyj, Helsinki, Finland). The gravimetric mass concentration was determined by sampling a major fraction of the excess aerosol on a Teflon R2PJ047 filter (Pall corp., Ann Arbor, MI) and measuring the volume of the collected aerosol (the inhaled minute volume of all mice was about 1% of the total aerosol flow). For filter weighing, a Sartorius MC-5 microbalance (Sartorius, Goettingen, Germany) was used in controlled relative humidity (40–45%) and temperature ($21\text{--}23^\circ\text{C}$) conditions; to do the mass measurements, the filters were weighed before and after each exposure. Laboratory and field blanks were used for quality assurance.

In order to characterise the ultrastructure and elemental composition of nanoparticles, a drop of $25 \mu\text{L}$ of AgNP suspension recovered from a dedicated Teflon filter was spotted on formvar-coated copper grids and allowed to air dry for 2 h at room temperature energy-dispersive X-ray (EDX). EDX spectra were acquired with an EDX detector (Thermo Scientific, Waltham, MA) at an acceleration voltage of 75 KeV. Magnifications of 12,000 Spectra were semiquantitatively analysed by the Noram System Six software (Thermo Scientific, Waltham, MA) using the standardless

Cliff–Lorimer k-factor method (Scimeca et al., 2014; Scimeca et al., 2016).

Tissue collection

Immediately before sacrifice about 100–150 µl of blood was collected through the orbital sinus membrane using a glass capillary, after local application of a drop of anaesthetic (proparacaine or tetracaine hydrochloride, according to availability). Blood was centrifuged at 3000 rpm for 5 minutes and serum was collected and stored at -80°C until use. Uteri were collected and analysed for the presence of resorptions, and placentas and foetuses harvested. Placentas and foetuses were counted, measured and weighed using an analytical balance (Sartorius, Italy).

For each female, foetuses, resorptions, placentas and maternal tissues, including lung, liver, spleen, kidney and mammary gland, were equally divided and processed for the planned analyses. Specifically, for TEM/EDX analysis and histological evaluation, samples were washed in PBS, transferred in a 4% paraformaldehyde solution and processed as below reported; for single-particle ICP-MS analysis, samples collected in clean tubes were stored at -80°C until further processing (see specific section); for protein and RNA extraction, tissues were immediately flash frozen in liquid nitrogen and stored at -80°C until use.

Identification of nanoparticles in tissues through TEM/EDX analysis

For each mouse, we analysed one cubic millimetre of the following specimens: superior lobe of the right lung (two samples), liver (right anterior, right posterior, caudate, median and left lobules), spleen (marginal and core zone), placenta (maternal side, maternal–foetal interface, foetal side), foetus (two fragments from the caudal region, two fragments from the central body and two fragments from the cephalic region) and embryonic resorption (ten fragments randomly selected). Tissues were fixed in 4% paraformaldehyde and post-fixed in 2% osmium tetroxide (Hayat, 1981). After washing with 0.1 M phosphate buffer, the sample was dehydrated by a series of incubations in 30%, 50% and 70% ethanol. Dehydration was continued by incubation steps in 95% ethanol, absolute ethanol and propylene oxide, after which samples were embedded in Epon (Agar Scientific, Stansted, Essex, United Kingdom) (Hayat, 1981). Eighty nanometre ultra-thin sections were mounted on copper grids, stained with uranyl acetate and lead citrate, and examined with a transmission electron microscope (Model 7100FA, Hitachi, Schaumburg, IL). For the EDX microanalysis, 100-nm-thick unstained ultrathin sections were placed on copper grids. The EDX spectra were acquired by a Hitachi 7100FA transmission electron microscope and an EDX detector (Thermo Scientific, Waltham, MA) at an acceleration voltage of 75 KeV and 12,000 magnification. Specifically, AgNPs were detected at 30–100,000 magnifications, and then the area of interest was analysed by EDX analysis at 12,000 magnifications by focussing the electron beam in correspondence with the suspicious AgNPs. Spectra were semiquantitatively analysed as reported above.

Detection and quantification of Ag nanoparticles in tissues by single-particle ICP-MS

All procedures were carried out under clean room conditions. For the extraction of Ag NPs from whole organs, samples were added with a 20% wt solution of tetramethylammonium hydroxide (TMAH) TraceSELECT (Sigma-Aldrich, Darmstadt, Germany) according to a 20:1 volume to weight ratio and sonicated with a

Bandelin Sonopulse HD 3200 apparatus equipped with a MS72 tapered tip at 38 W for 5 minutes in pulse mode ($6\text{ s} + 2\text{ s}$ cycles). Samples were mechanically shaken overnight at room temperature and then diluted with ultrapure water for single-particle ICP-MS analysis. Procedural blanks were run in parallel.

Analysis of samples extracts by single-particle ICP-MS was performed using a Nexion 350D ICP-MS apparatus (PerkinElmer, Waltham, MA) equipped with a quartz concentric nebuliser and a cyclonic spray chamber (Waltham, MA). The sample flow rate to the nebuliser was set at 0.5 mL/min and checked daily by a flow meter (SEDNA, EPOND, Effretikon, Switzerland). Data acquisition (analytical mass 107Ag) was performed using the Syngistix Nano Module with a dwell time of 0.1 ms and an acquisition time of 60 s per measurement. Data were processed for calculation of particle sizes, particle size distribution, particle number concentration and particle mass concentration assuming a spherical particle shape. A reference Au NP suspension of 60 nm nominal diameter (RM8013) obtained from NIST (Gaithersburg, MD) was used as particle size calibration standard. The calibration for Ag was performed with an ionic Ag standard for ICP-MS (High Purity Standard, Charleston, SC). After the analysis of each sample, ultrapure water was analysed to check the absence of carryover from the previous measurement. A commercial suspension of 20 nm Ag NPs (Sigma-Aldrich, Darmstadt, Germany) was used to assess the particle recovery rate after TMAH extraction ($n = 3$). Recovery was assessed by comparing the Ag NP number and mass distributions in digested spiked samples and in ultrapure water. The number-based recovery of Ag NPs extracted from the spiked sample was $87 \pm 12\%$, while the mass-based recovery was $102 \pm 15\%$. The size detection limit of single-particle ICP-MS analysis was 13 nm, while the mass concentration detection limit was $\sim 0.001\text{ mg/kg w.w.}$

Since the TMAH treatment gives results comparable to acidic digestion (Bolea et al., 2014; Gray et al., 2013), Ag in the TMAH extracts was determined by conventional ICP-MS in parallel with single-particle measurements to quantitate total Ag (sum of particulate and ionic silver) in samples.

Histological analysis

After fixation in 4% paraformaldehyde overnight at 4°C , tissues were washed in PBS and dehydrated in increasing concentrations of ethanol for paraffin embedding, following standard procedures. Eight micrometre sections were deparaffinised and stained in haematoxylin and eosin, according to standard protocols. Images were acquired using a Zeiss Axioplan 2 microscope connected to a Nikon digital camera, using the NIS-Element software.

Gene expression analysis through quantitative RT-PCR

Total RNA was isolated from frozen tissue samples using TRIzol[®] (Invitrogen; Thermo Fisher Scientific, Inc., Waltham, MA) according to the manufacturer's protocol. RNA quality was examined on agarose gels. Synthesis of cDNA was performed using the QuantiTect Reverse Transcription Kit (Qiagen, Hilden, Germany) following the manufacturer's specifications. This kit included treatment of RNA samples with DNase I. qRT-PCR was performed using an Applied Biosystems 7300 Real Time PCR System (Applied Biosystems; Foster City, CA) with KAPA SYBR FAST qPCR (Kapa Biosystems, Wilmington, MA). All samples were run in triplicate and average values were calculated. Each qRT-PCR experiment was repeated three times. Analysis of relative gene expression data was performed using the $\Delta\Delta\text{CT}$ method and normalised to glyceraldehyde 3-phosphate dehydrogenase (GAPDH). Specific primers for IL-6, MCP-1, TNF- α and IL-1 β were designed using Primer

Express® software v2.0 (Applied Biosystems); sequences are listed below:

IL-6 Fw: 5'-GTTCTCTGGGAAATCGTGA-3'
 IL-6 Rv: 5'-ACGATGATGCACTTGACAGAA-3'
 MCP-1 Fw: 5'-AGGTGTCCCAAGAAGCTGTA-3'
 MCP-1 Rv: 5'-ATGTCTGGACCCATTCTTCT-3'
 TNF- α Fw: 5'-CCCCAAAGGGATGAGAAGTTC-3'
 TNF- α Rv: 5'-TGAGGGTCTGGGCCATAGAA-3'
 IL-1 β Fw: 5'-TCAGGCAGGCAGTATCACTC-3'
 IL-1 β Rv: 5'-CTAATGGGAACGTCACACC-3'
 GAPDH Fw: 5'-AACTTTGGCATTGTGGAAGG-3'
 GAPDH Rv: 5'-CACATTGGGGGTAGGAACAC-3'

Oestrogen serum level determination

In order to determine the levels of oestrogen in blood serum of pregnant and non-pregnant females, a Mouse/Rat Estradiol ELISA kit (Sigma-Aldrich) was used, according to the manufacturer's protocol. Briefly, 25 μ l of mouse E2 standard or mouse serum and 100 μ l of oestradiol enzyme conjugate were added to the anti-E2 polyclonal antibody-coated wells and incubated for 120 min at

room temperature. Following 3 washes, horseradish peroxidase-conjugated detection antibodies were added, followed by the substrate solution. The absorbance of each well was measured at 450 nm using a microplate reader (Model 3550-UV, Bio-Rad, Hercules, CA).

Statistical analysis

Data provided in text and figures are means \pm SEM. Results were analysed using the chi-squared test, one-way analysis of variance (ANOVA) and Tukey's *post hoc* test (SigmaStat, Systat Software Inc., Richmond, CA). When $p < .05$, the analysis was considered significant.

Results

Exposure characterisation

In Figure 1(A), the statistics of the dimensional characteristics of the aerosol inhaled by the mice during the experiments are reported. The average number, surface area, volume and mass concentrations resulted equal to $3.80 \pm 0.33 \times 10^7$ part./cm³, $3.94 \pm 0.70 \times 10^{10}$ nm²/cm³, and $1.41 \pm 0.39 \times 10^{11}$ nm³/cm³, 642 ± 12.6 μ g/m³, respectively. Daily monitoring of the above-mentioned parameters showed quite constant exposure of the mice throughout the entire experimental analysis. The particle size

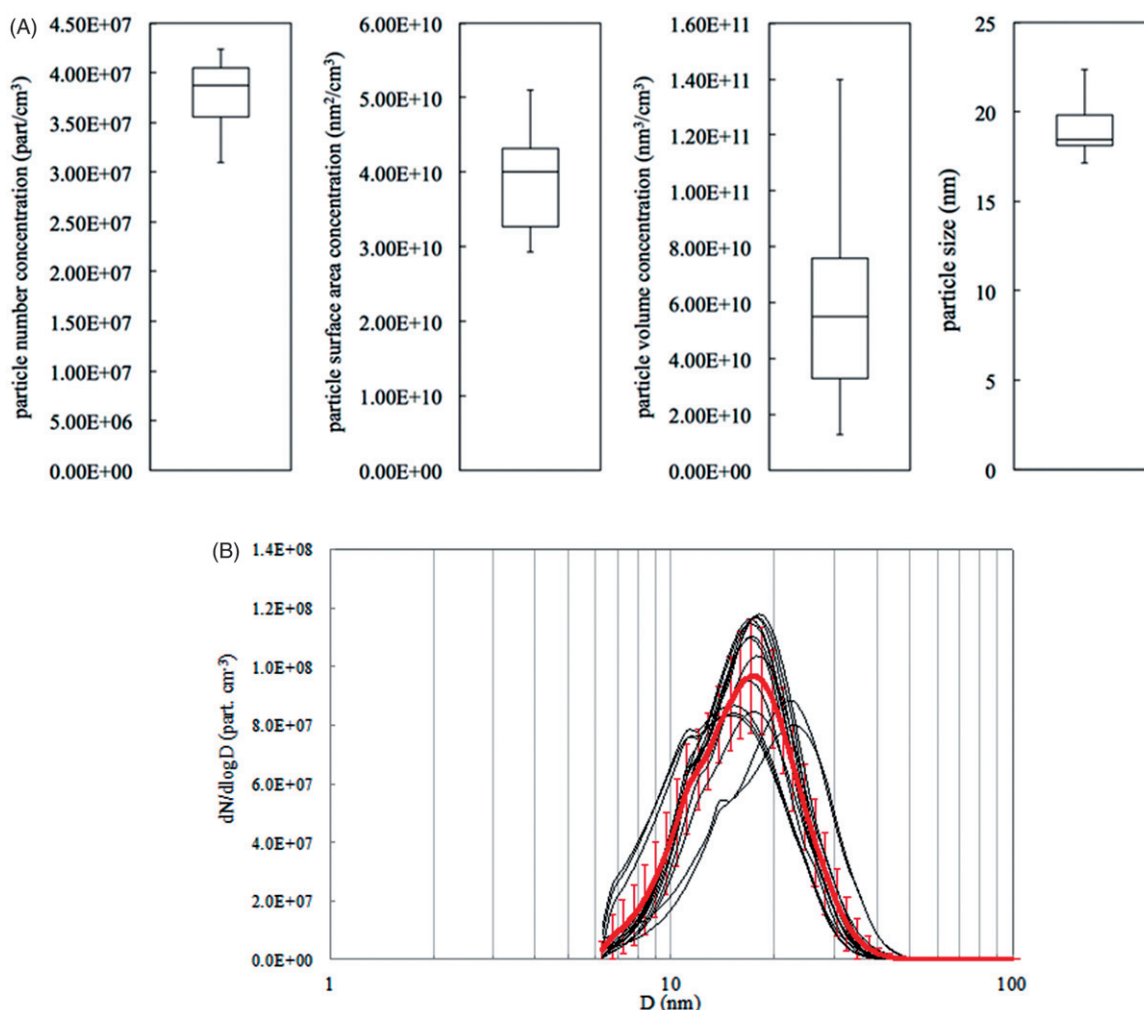


Figure 1. Characteristics of the aerosol inhaled by mice during the 4 h exposure. (A) Box plots of different aerosol metrics (particle number, surface area, volume concentrations and size). (B) Daily integral particle number distributions; the red bolt curve is the mean of all spectra.

distribution, shown in Figure 1(B), resulted unimodal with an average mode equal to 19.3 ± 2.3 nm. Analyses of the aerosol parameters shown in Figure 1(A) for the entire 4 h exposure period (exposure duration of the 4 h/d exposure group) were not statistically different from those during the first hour (exposure duration of the 1 h/d exposure group). Similarly, the size spectra shown in Figure 1(B) (referred to the 4 h period) were not statistically different between both exposure groups. Hence, both groups (1 h/d and 4 h/d exposure) received the same aerosol either for one hour or for four hours, and the exposure dose differed by a factor of four.

Figure 2 shows that the daily AgNPs mass concentration (mg/m^3) determined from daily collected AgNP aerosol filters was fairly constant over the entire exposure period. From these mass concentration data and the volume concentration data determined by Scanning Mobility Particle Sizer (SMPS), the effective density of the AgNPs averaged over the entire exposure period was estimated to be $4.9 \text{ g}/\text{cm}^3$. This means that the AgNPs showed a density lower than that of bulk silver ($10.5 \text{ g}/\text{cm}^3$) and indicates that melting in the tube furnace immediately after their generation by the spark ignition generator did not yield completely dense single spherical AgNPs which was supported by the transmission electron microscopy (TEM) images shown in Figure 3(A). EDX analysis confirmed that nanoparticles collected from the generator were made of silver (Figure 3(B)).

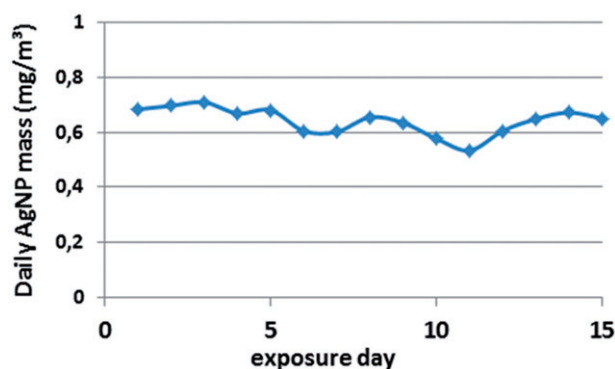


Figure 2. Daily AgNP mass concentration (mg/m^3) determined from daily collected AgNP aerosol filters after the 4 h exposure period.

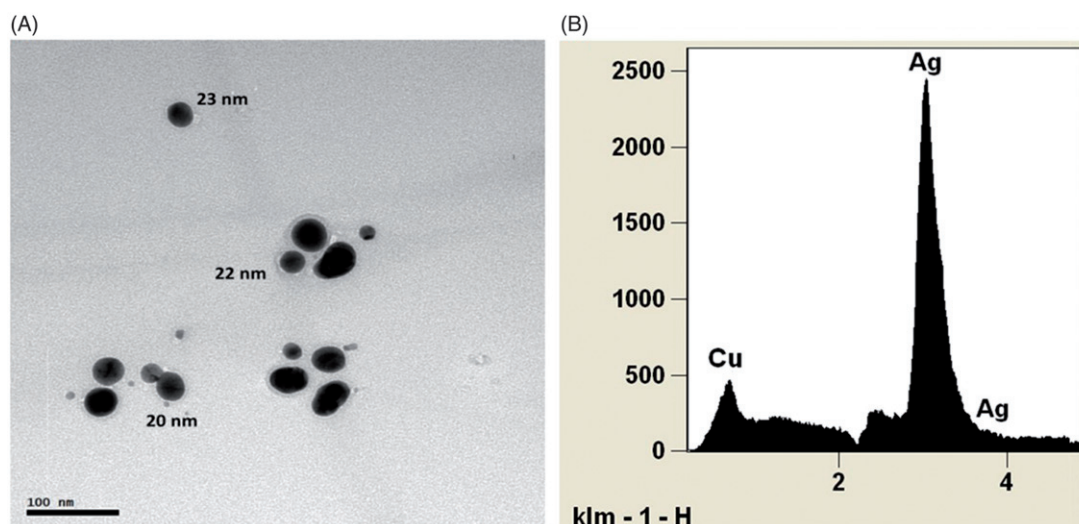


Figure 3. (A) Representative transmission electron micrograph showing the freshly produced AgNPs. (B) Energy-dispersive X-ray (EDX) spectrum of the NPs shown in (A), confirming that nanoparticle composition consisted in elemental silver.

The accumulating deposited AgNPs mass in the lungs was modelled using the MPPD software (Multiple-Path Particle Dosimetry Model, ARA, version 3.04, www.ara.com; Miller et al., 2016), based on the aerosol parameters given above and the following physiology parameters: mouse nose-only inhalation, head volume 0.04 mL, equal fractions of inspiration and expiration without any pause. In order to estimate changes in deposition, additional parameters were varied in the following range: tidal volume (0.15, 2.0, 2.4 mL), breathing frequency (120, 160, 200 #/min) and functional residual capacity (0.4, 0.6, 0.8, 1.0 mL). About half of the inhaled AgNP aerosol deposited in the murine respiratory tract, but only about 15% deposited in the alveolar region and the remaining 35% deposited in head and conducting airways.

In Figure 4, the accumulating AgNPs mass is shown for the alveolar region since deposition in the airways of head and conducting thoracic airways was eliminated from the lungs within 24 h after deposition. At the end of exposure, an accumulated dose of 270 mg/kg (lung weight) was estimated. In addition, the long-term macrophage-mediated clearance (LT-MC) from the alveolar region was subtracted assuming a daily clearance rate of 0.0215/d of the contemporary lung burden (Kreyling, 1990; Semmler-Behnke et al., 2004; Semmler-Behnke et al., 2007). After 14 days, about 17% of the deposited AgNP were cleared by LT-MC. Median values and 25% and 75% interquartile range from the estimates over the ranges of the varied parameters are presented.

The estimated AgNP accumulation is compared to the measured AgNP contents of the lungs of the 4 h exposure group on day 15 measured by inductively coupled plasma mass spectrometry (ICP-MS). The estimated accumulation agrees reasonably well, but the estimate is systematically, slightly higher than the experimental data. This may have been caused by the parameters chosen for the modelling and/or it could reflect partial dissolution of the AgNPs and the additional clearance of dissolved Ag from the lungs.

NP biodistribution in maternal and foetal tissues

TEM analysis confirmed deposition of AgNPs in the lung tissue of the exposed animal (Figure 5(C)). Nanoparticles were identified in the alveolar space of both 1 h/d and 4 h/d AgNP-exposed groups,

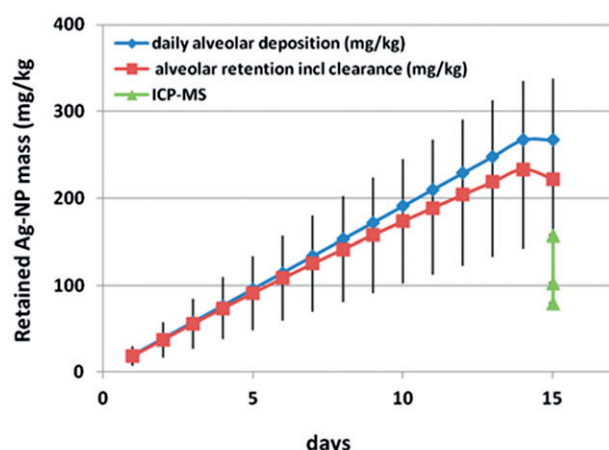


Figure 4. Accumulating AgNPs mass is shown for the alveolar region (diamond) during the 15-day exposure period. At the end of exposure, an accumulated dose of 270 mg/kg (lung weight) was estimated. In addition, the long-term macrophage-mediated clearance (LT-MC) from the alveolar region was subtracted (square) assuming a daily murine clearance rate of 0.022/d of the contemporary lung burden (Kreyling, 1990; Semmler-Behnke et al., 2004; Semmler-Behnke et al., 2007). Median values and 25% and 75% interquartile range of the estimates are shown for the varied physiology parameters: tidal volume (0.15, 2.0, 2.4 mL), breathing frequency (120, 160, 200 #/min); functional residual capacity (0.4, 0.6, 0.8, 1.0 mL). In addition, the experimentally determined Ag mass in individual mice determined by ICP-MS is shown at day 15 in the lungs of the 4 h/d exposed group.

while no particle-like structures were observed in the lung from clean air-exposed mice (Figure 5(A)).

Quantitative results of AgNP tissue distribution were obtained for the 4 h/d exposure groups by single-particle ICP-MS. Results are summarised in Table 1. Mass concentration of AgNPs in lungs was 24.3 ± 18.5 mg/kg of tissue, and the percentage of particles with a diameter above the size detection limit (estimated to be around 13 nm) was consistently around 20%. AgNPs were not detected in control samples (average mass concentration below the detection limit).

Silver nanoparticles were also identified and quantified in tissues across the air-blood barrier, such as liver, spleen and placenta. No particles were detected in control samples, while in the organs of the 4 h/d NP-exposed animals, mass concentration was in the order of micrograms per kilogram of tissue (Table 1). In particular, in the placenta the total mass concentration of AgNPs was 0.005 ± 0.001 mg/kg, and the amount of total silver was 0.082 ± 0.006 mg/kg. In foetuses, a very low number of particles were present, but the amount was collectively below the detection limit (Table 1). However, the total silver content detected in foetuses was 0.012 ± 0.003 mg/kg, part of which probably included AgNPs sized ≤ 13 nm.

The presence of silver as nanoparticle in tissues beyond the lung barrier was confirmed by TEM. Particle-like structures were identified in the liver, in lysosomal-like vesicles (Figure 5(D)), where the presence of silver was confirmed by EDX (Figure 5(E,F; E spectrum of C; F spectrum of D)). No silver was detected in control tissues, and the particle-like structures observed in hepatocytes resembled glycogen granules (Figure 5(B), control). AgNPs were also identified in placental tissue. Specifically, in the foetal side of the placenta, we observed nanoparticles in close proximity to the trophoblast cells (Figure 6(C)), which are the main cell type that separates the foetal vasculature from the maternal blood, and into degenerating mitochondria within trophoblast cells (Figure 6(B)). Moreover, we observed that NPs were frequently decorating maternal blood cells (Figure 6(D)); the silver content of the identified particles was confirmed each time by EDX analysis

(Figure 6(E,F; E spectrum of B; F spectrum of C)). Although in foetuses the amount of silver as nanoparticles measured by single-particle ICP-MS (SP-ICP-MS) was collectively below the detection limit, TEM analysis allowed to identify nanoparticle-like structures in the head region of the foetus. Figure 6 (G,H) shows NPs contained in the cytoplasm of a foetal endothelial cell and in mitochondria. Silver content of these particles was confirmed by EDX (Figure 6(I), spectrum of H).

Twenty nanometre-sized particles were identified by TEM also in the intercellular space of degenerated embryo-placental structures from 4 h/d exposure group dams, and silver was detected by EDX in lysosome-like structures within cells, where possibly nanoparticles encountering dissolution were present (Figure 6(J-L)).

Toxicological study

Histopathological analysis of maternal liver and spleen did not show major morphological alterations between control and AgNP-exposed mice, beside sporadic sites of fatty degeneration (steatosis) in liver from the 4 h/d exposure group (Figure 7(B)). Minor tissue alterations were observed in kidneys from the 4 h/d exposure group, where dilation of periglomerular space of the Bowman's capsule was evidenced after H&E staining of kidney sections (Figure 7(D)). In non-pregnant mice, none of the minor tissue alterations observed in pregnant animals were detected (not shown).

Analysis of the effects of inhalation exposure to AgNP on pregnancy outcome demonstrated no significant changes in maternal weight gain during the first 15 days of pregnancy within the three groups (not shown), nor differences in the number of foetuses per dam or foetal cranial to caudal length and weight (Table 2). Histopathological analysis of the placentas demonstrated that there were no significant and treatment-related morphological abnormalities in the structural organisation of both foetal and maternal side of the tissue (not shown). The effect of maternal inhalation exposure to AgNPs consisted in a statistically significant increase in the number of foetal resorptions in the 4 h/d exposure group (Table 2).

To explain the observed increased number of degenerated conceptuses, we measured oestrogen levels in maternal serum, since levels of this hormone are fundamental for the maintenance of a healthy pregnancy. In the serum of pregnant females, oestradiol appeared significantly decreased only in the 4 h/d exposure group (Figure 8(A)). Interestingly, oestrogen was also decreased in the serum of non-pregnant females (all in the same phase of the oestrus cycle) that were exposed in parallel with the other groups (Figure 8(B)).

Inflammation as a consequence of AgNP inhalation was also investigated. In the lung of exposed dams, expression of inflammatory mediators, such as IL-6, IL-1 β , TNF- α and MCP-1, was significantly up-regulated, and for the first three genes, up-regulation was highest in the 4 h/d exposure group (Figure 9(A)). Similarly, in placentas we observed a significant increase in the expression of TNF- α , which is considered a key mediator of placental inflammation (Figure 9(B)). This was also accompanied by an increase in the expression of IL-1 β , produced by the macrophages infiltrating the placenta during the inflammatory response.

Discussion

The relevance of investigating the effect of maternal exposure to engineered nanoparticles during pregnancy has recently emerged; however, there is still a shortage of data regarding the effects exerted after inhalation exposure, as recently highlighted by a

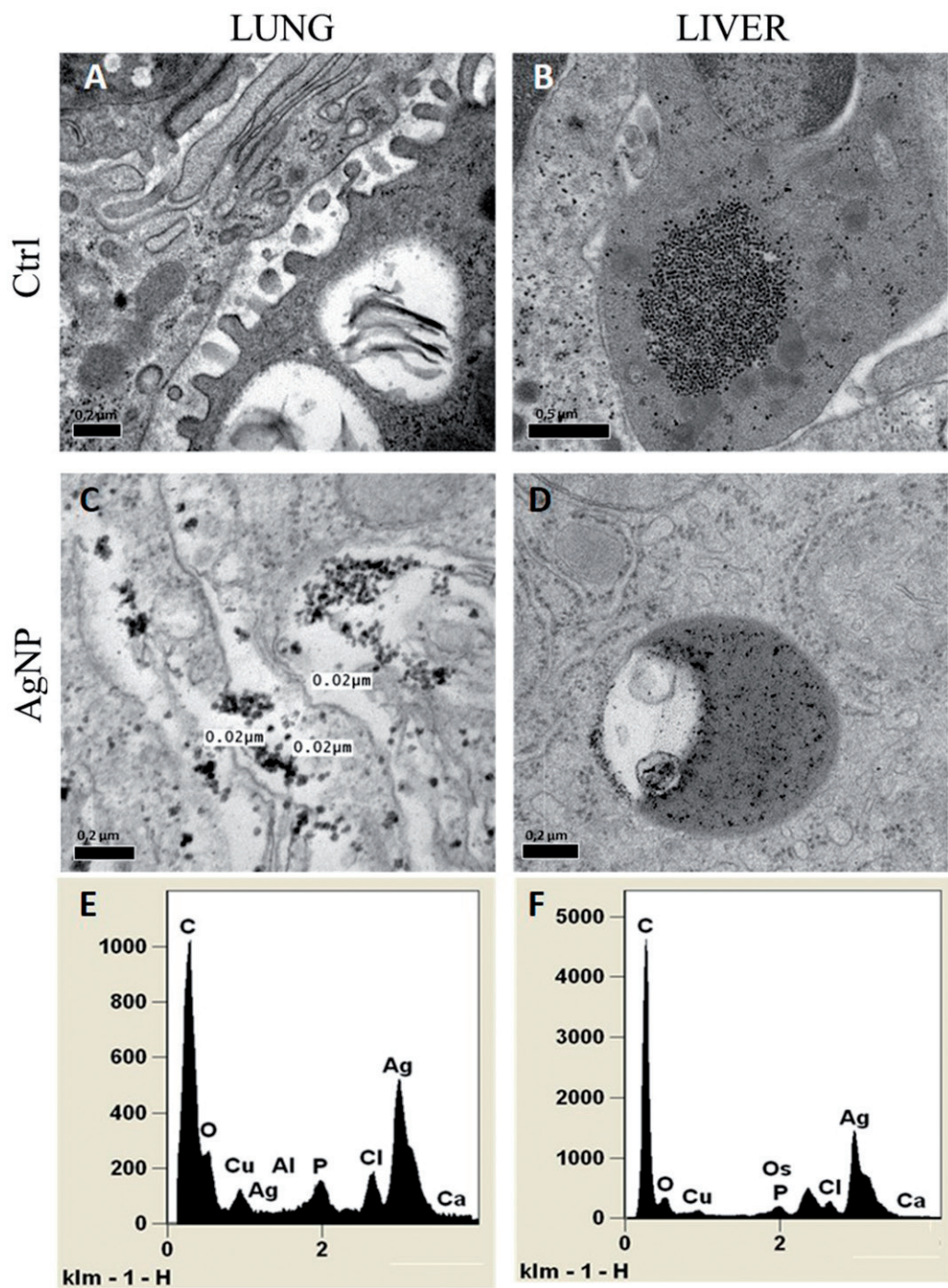


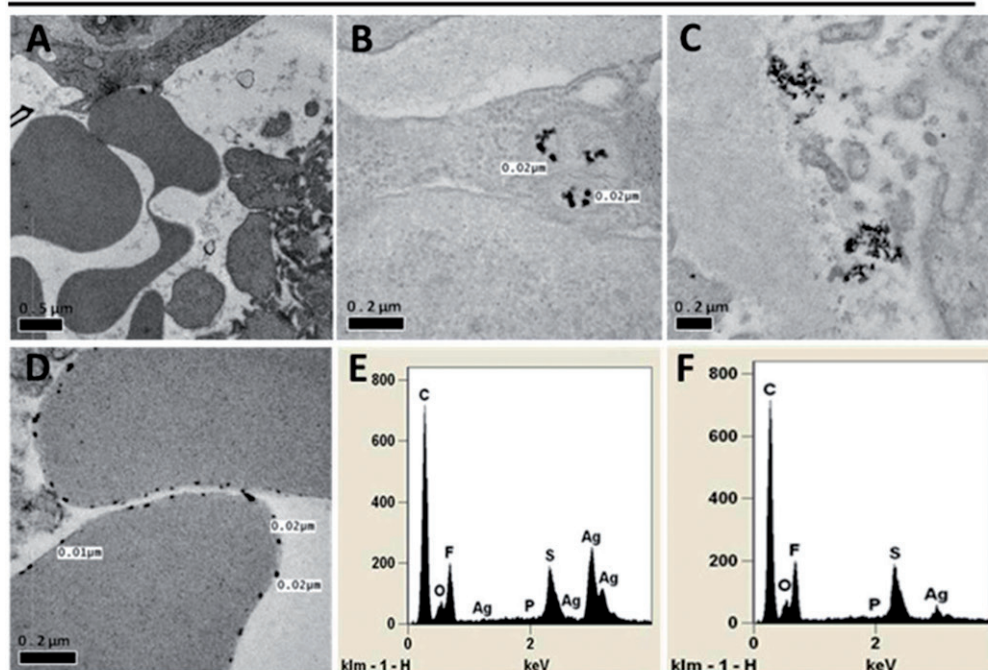
Figure 5. Transmission electron microscopy (TEM) analysis of maternal lung (A,C) and liver (B,D). (A–C) Representative TEM images of maternal lung from control (A) and 4 h/d exposure group (C), with relative energy-dispersive X-ray (EDX) spectrum (E). (B–D) Representative TEM images of maternal liver from control (B) and 4 h/d exposure group (D), with relative EDX spectrum (F).

Table 1. Quantitative results for the tissue distribution of Ag NPs obtained for the 4 h/d exposure group by SP-ICP-MS, expressed on a wet weight basis (*n* = 3). The ranges of measured values are shown in brackets.

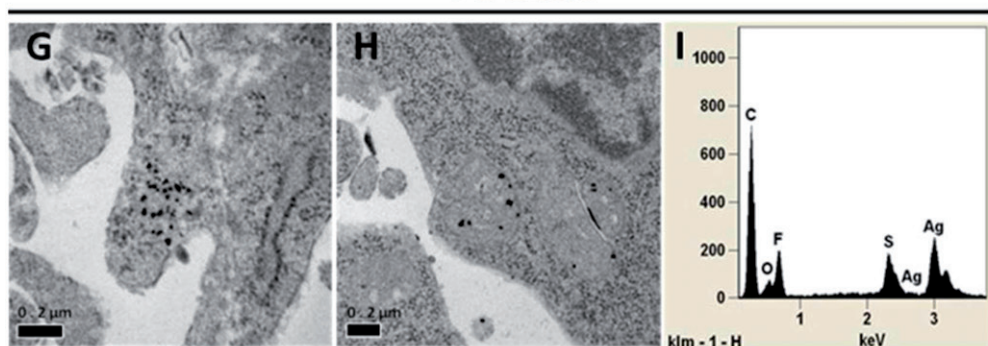
	Size, mode [nm]	Size, mean [nm]	Particle number conc. [# parts/g]	Particle mass conc. [mg/kg]	<size DL & ionic Ag mass conc.	Total Ag ^a [mg/kg]
Lungs	19 ± 2 (17–21)	26 ± 2 (23–28)	2.0 × 10 ¹¹ ± 2.1 × 10 ¹¹ (6.5 × 10 ¹⁰ –4.5 × 10 ¹¹)	24.3 ± 18.4 (12.3–45.5)	84.8 ± 16.8 (66.9–100.2)	114.1 ± 42.2 (79.2–160.8)
Spleen	19 ± 3 (17–22)	25 ± 4 (21–28)	2.1 × 10 ⁸ ± 2.2 × 10 ⁸ (3.9 × 10 ⁷ –4.6 × 10 ⁸)	0.028 ± 0.038 (0.006–0.072)	0.168 ± 0.034 (0.143–0.207)	0.197 ± 0.071 (0.151–0.279)
Liver	16 ± 1 (16–18)	22 ± 2 (20–24)	2.4 × 10 ⁸ ± 9.2 × 10 ⁷ (1.4 × 10 ⁸ ± 3.1 × 10 ⁸)	0.016 ± 0.008 (0.007–0.023)	0.120 ± 0.006 (0.116–0.126)	0.135 ± 0.011 (0.123–0.143)
Placenta	19 ± 1 (18–19)	23 ± 1 (23–24)	6.4 × 10 ⁷ ± 1.9 × 10 ⁷ (5.5 × 10 ⁷ ± 8.6 × 10 ⁷)	0.005 ± 0.001 (0.004–0.006)	0.077 ± 0.009 (0.067–0.085)	0.082 ± 0.010 (0.071–0.091)
Embryos	<LOD	<LOD	<LOD	<LOD	0.011 ± 0.006 (0.004–0.016)	0.012 ± 0.006 (0.005–0.017)

^aIndependently determined by conventional ICP-MS, it is the sum of the mass concentration of measured particles and particles < size DL along with ionic silver.

Placenta



Foetus



Resorption

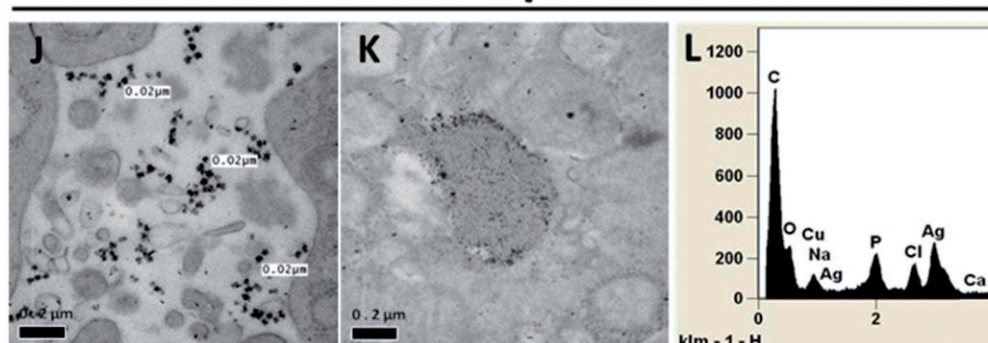


Figure 6. Representative images of transmission electron microscopy (TEM) analysis performed on placenta, foetuses and resorptions from control and exposed mothers. (A–F) Representative placenta TEM images from control (A), 1 h/d exposure group (B) and 4 h/d exposure group (C,D), with relative energy-dispersive X-ray (EDX) spectra (E spectrum of B; F spectrum of C), confirming the silver content of the particles identified by TEM analysis. (G–I) Representative TEM images from foetuses of longer exposed mothers (G,H), showing the presence of nanoparticles in the head region; silver content of these particles was confirmed by EDX analysis (I). (J–L) Representative TEM images of resorptions of longer exposed mothers (J,K), with the relative EDX analysis (L).

comprehensive review on this topic (Hougaard et al., 2015). To our knowledge, this is the first report demonstrating that inhalation exposure to silver nanoparticles results in accumulation of nanoparticles in the placenta and in foetal tissues and induces an

adverse pregnancy outcome. In our study, the 1 h/d exposure group had a daily exposure of 0.64 mg/m^3 for 1 h, which is in the range of the allowed daily exposure in humans (0.1 mg/m^3 for 8 h) (SCENIHR, 2014). However, it has been recently suggested to

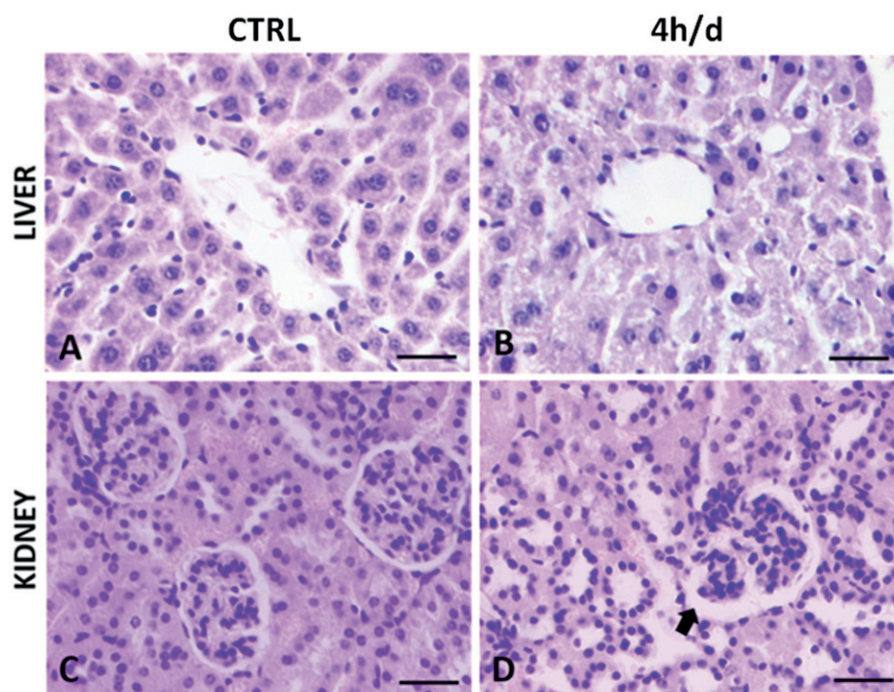


Figure 7. Histopathological analysis of maternal tissues. (A,B) Representative liver sections from control (A) and 4 h/d exposure dams (B), evidencing no specific lesions of the tissue, except for diffuse areas of steatosis in the 4 h/d exposure liver section. (C,D) Representative kidney sections from control (C) and 4 h/d (D) exposure dams, demonstrating the presence of increased periglomerular space in the glomeruli of the longer exposed group (arrow). Scale bars = 30 μ m.

Table 2. Summary of the main pregnancy outcomes after inhalation exposure to AgNP for 15 days.

	Dams	Foetuses/female	Crown-rump length	Foetal weight (mg)	Resorptions	% resorp./tot events	% females with resorptions
CTRL (4h air)	4	8.0 \pm 1.5	0.90 \pm 0.18	180 \pm 42.8	1	3%	25%
1h/d Exposure	4	7.0 \pm 0.4	0.95 \pm 0.20	164 \pm 14.6	5	15%	75%
4h/d Exposure	5	5.2 \pm 1.8	1.00 \pm 0.11	159 \pm 20.2	13*	33%	80%

*Statistically significant versus control ($p < .0001$) and 1 h/d exposure group ($p < .02$).

consider whether the relatively small translocation proportions identified in rodents might be greater in humans (Stone et al., 2016). On this basis, in order to simulate a possible higher translocation rate in humans at the allowed exposure doses, we exposed one group of pregnant mice also to a fourfold higher dose of AgNPs. This was achieved by increasing the exposure duration per day, avoiding a shift in size distribution that often takes place when increasing the particle numbers. Estimating the deposited AgNP mass in a healthy adult human provides a similar slope as shown in Figure 4, but results in an accumulated AgNPs mass of 0.075 mg/kg in the total respiratory tract and 0.037 mg/kg in the alveolar region. However, since LT-MC is tenfold slower in man than in mice, the resulting curve would only be about 2% lower (Kreyling, 1990; Semmler-Behnke et al., 2004).

In the present study, we observed the presence of silver-containing particles in lungs and in tissues beyond the air-blood barrier, in both the 1 h/d and 4 h/d exposure groups. Not surprisingly, nanoparticles were identified in liver and spleen of both 1 h/d and 4 h/d exposure groups by TEM associated with EDX and single-particle ICP-MS analysis, as previously reported by others (Davenport et al., 2015; Gosens et al., 2016; Lebedová et al., 2016). Importantly, our analysis also allowed identifying for the first time silver-containing nanoparticles in the placenta after maternal inhalation exposure. The combination of TEM and EDX analysis was of major importance to indisputably establish the chemical nature of the observed nanoparticle-like structures. In fact, we identified nanoparticle-like structures of a size similar to the produced silver nanoparticles in both control and Ag-exposed animals. EDX analysis confirmed the presence of silver in the

AgNP-exposed groups only. Single-particle ICP-MS analysis allowed to quantitating silver present as nanoparticles. In particular, the mass of silver present in the placenta as nanoparticles was estimated to be about 0.02% of the amount detected in lungs, suggesting that nanoparticles, and not only the soluble ions, are able to cross the air-blood barrier, and reach the highly vascularised foetoplacental unit. This was further confirmed by our TEM/EDX analysis, which allowed the visualisation of silver nanoparticles of the expected size in both placenta and foetus. We cannot unequivocally rule out the possibility that some of the nanoparticles identified in tissues are not primary particles that translocated the lung barrier. Indeed, secondary nanoparticles formed after interaction of the released silver ions with sulphur groups of proteins, and/or selenium or chloride present in tissues might very well have occurred, as recently suggested (Juling et al., 2016). By ICP-MS analysis, we also quantitated the total silver content in tissues. This included released ions, nanoparticles in the size range shown in Figure 1(B) (see Figure 1(B)), as well as partly dissolved nanoparticles (with size below the 13 nm detection limit of single-particle ICP-MS). Interestingly, the mass concentration ratio of silver nanoparticles over total silver differs between lung and internal organs, and among the different internal organs (Table 1). Specifically, in the embryo, the detected silver was almost entirely in the ionic form or as NP < 13 nm. In the placenta, AgNPs were about 6% of the total Ag, while in the liver and spleen, the percentage was about twice this value (12% and 14%, respectively). By comparison, in the lung 21% of the total Ag was still in the particulate form at the time of the measurements. From these data, we can infer that silver translocating from the

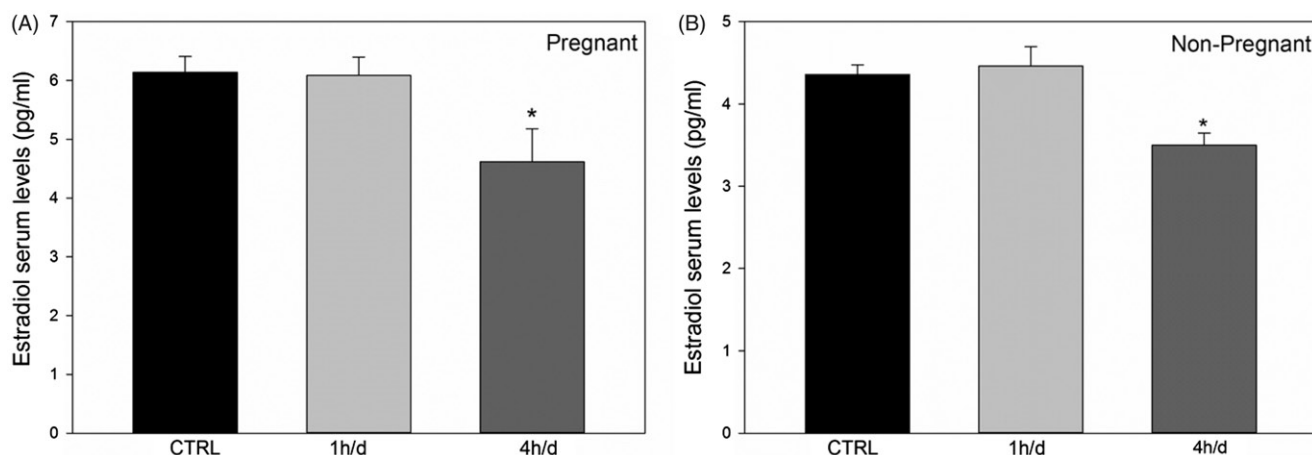


Figure 8. Quantification of maternal serum levels of oestrogens in (A) pregnant and (B) non-pregnant mice after 1 h/d and 4 h/d exposure to AgNPs.

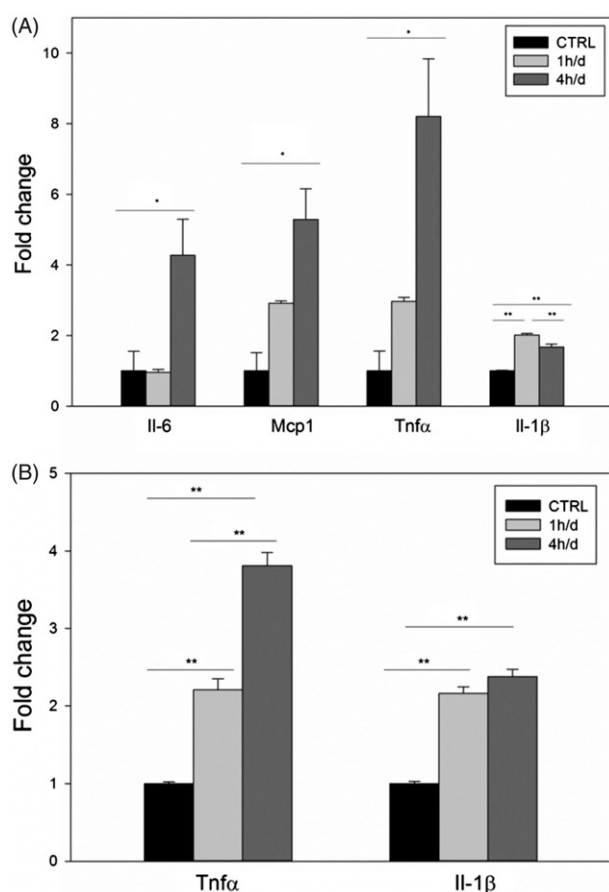


Figure 9. Gene expression analysis of inflammatory cytokines in (A) lung and (B) placental tissue. * $p < .05$; ** $p < .005$.

lung is mainly ionic – or in the form of small, readily dissolving particles – and same is true for the fraction translocating the second barrier, i.e., the placenta. In fact, SP-ICP-MS analysis failed to detect nanoparticles in the foetus, which may be due to the limit of detection, as suggested by the presence of Ag-containing particles identified by TEM/EDX analysis. Irrespective of that, very little silver will be transported to the foetus upon inhalation.

To the best of our knowledge, no data of transplacental passage of AgNP, after maternal inhalation exposure, have been reported before. For other nanoparticles, such as polystyrene, CuO and CdO, no placental translocation has been detected by ICP-MS

(Adamcakova-Dodd et al., 2015; Blum et al., 2012; Huang et al., 2015; Muoth et al., 2016), even for CdO particles as small as 15 nm (Blum et al., 2012). Since negligible dissolution was reported for these NPs (Blum et al., 2012), this suggests that NPs of this size and chemistry are not able to cross the placental barrier, or at most do so at extremely low percentages of the delivered dose. Concerning CuO NPs, no differences in placental and foetal accumulation were observed between exposed and non-exposed pregnant mice by ICP-MS (Adamcakova-Dodd et al., 2015). However, as reported by the authors, Cu levels in blood of both groups doubled during pregnancy. Therefore, the entity of such a physiological change might obscure any possible translocation of the inhaled CuO, which is estimated to be about 1% of the pulmonary-deposited dose (Gosens et al., 2016). To assess the possibility that AgNPs or released ions might reach the foetus, we have used a complementary approach, which was fundamental for a correct interpretation of the SP-ICP-MS results. In fact, by TEM associated with EDX analysis, we were able to identify AgNPs with a size in the range of the particles produced in our study, thus suggesting that total silver detected by ICP-MS included also a possibly very low fraction of nanoparticles.

Although we have applied a high pulmonary dose to the mice, we did not observe major pathological changes in the lung of the mothers in both the 1 h/d and 4 h/d exposure groups. This is in line with what has been previously reported by Sung et al., who did not detect any histopathological change in lungs of rats exposed for 65 days at $133 \mu\text{g}/\text{m}^3$, and minimal changes in rats exposed to $515 \mu\text{g}/\text{m}^3$ for the same duration (Sung et al., 2009), concentrations that were comparable to those used in our study. Also, Smulders et al. reported minimal toxicity based upon an accumulated dose of 0.1 mg (Smulders et al., 2014). Of note, lung tissue in rats is more sensitive to inhalation of metal nanoparticles than in mice (Bermudez et al., 2004), and this may explain why we were unable to detect even minimal changes in our model. Minor lesions were detected in organs beyond the lung epithelial barrier, such as liver and kidney. Specifically, in the 4 h/d exposure group, we identified focal hepatic steatosis in liver and enlargement of the Bowman's space in kidney, thus confirming that liver and kidney may be a target for nanoparticle toxicity (Iavicoli et al., 2016). Interestingly, no glomerular damage was observed in kidneys from non-pregnant exposed females (not shown), suggesting a specific pregnancy-related toxic effect in this organ. This might be explained by the expansion of blood volume in the kidneys during pregnancy, which might carry a higher load of NP to the glomeruli.

Concerning the effects on pregnancy, we detected a statistically significant increase in the number of early resorbed fetuses in the 4 h/d exposure group, while only a slight non-significant increase was observed in the 1 h/d exposure group. We cannot exclude, however, that the lack of significant effect in the short exposure group might be partly linked to the lower number of dams analysed. In fact, the percentage of dams carrying at least one resorbed fetus was similar between the 4 h/d and 1 h/d exposure groups. The increased number of resorptions in the 4 h/d exposure group might be partly explained by the reduction of measured circulating oestrogen levels, indicating an endocrine disrupting action of the AgNPs at the higher dose. Although not assessed in this study, it is likely that other pregnancy-related hormones, such as progesterone and placental growth factor, might be affected by the exposure to nanoparticles. A stochastic distribution of nanoparticles in the uterus and/or a differential susceptibility of the different conceptuses may explain the survival of part of the fetuses. The lack of evident morphological alterations in the surviving fetuses, in spite of the observed presence of AgNPs, may be consequence of the very low amount of nanoparticles reaching the foetal tissues. We cannot exclude latent damage which could manifest later in gestation or postnatally, as reported for other nanoparticles (Adamcakova-Dodd et al., 2015; Engler-Chiurazzi et al., 2016). In this respect, it is relevant to stress that, although we did not observe histopathological changes in the placentas of both nanoparticle-exposed groups, we detected increased expression of pregnancy-relevant pro-inflammatory mediators, such as TNF- α and IL-1 β , that was more pronounced in the 4 h/d group. Increased expression of IL-1 β in the placenta has been associated with impaired cognitive functions in the progeny (Girard et al., 2010; Paris et al., 2011).

Conclusions

In conclusion, we have demonstrated that inhaled AgNPs may reach the placenta and the fetus, may cause damage to key maternal organs and affect pregnancy outcome, which may, at least in part, be related to the release of inflammatory mediators by the placenta. Since these results were derived from an exposure that might occur in humans, according to the current occupational limit values for metallic silver (Silver Nanotechnology Working Group, 2012), care should be taken in women of fertile age potentially exposed to AgNPs. This is of particular relevance for pregnancy outcome, considering that exposure at the very early stages (when pregnancy status might not be recognised) appears to be the most dangerous.

Acknowledgements

We would like to thank Roberta Bernardini for helping with blood sampling, Gabriele Rossi for assistance with histological procedures and Andrea Raggi for assistance with ICP-MS measurements.




Disclosure statement

The authors report no conflicts of interest.

Funding

This work has been supported by Finalized Health Projects of the Grant from the Italian Ministry of Health (RF-2009-1536665).

ORCID

Luisa Campagnolo  <http://orcid.org/0000-0003-3928-0276>
 Lucia Vecchione  <http://orcid.org/0000-0002-7984-6871>
 Manuel Scimeca  <http://orcid.org/0000-0003-0585-1309>
 Luca Stabile  <http://orcid.org/0000-0003-2454-0389>
 Francesco Cubadda  <http://orcid.org/0000-0003-3454-7947>
 Federica Aureli  <http://orcid.org/0000-0002-0601-5807>
 Wolfgang G. Kreyling  <http://orcid.org/0000-0002-0702-6567>

References

- Adamcakova-Dodd A, Monick MM, Powers LS, Gibson-Corley KN, Thorne PS. 2015. Effects of prenatal inhalation exposure to copper nanoparticles on murine dams and offspring. *Part Fibre Toxicol* 12:30.
- Bermudez E, Mangum JB, Wong BA, Asgharian B, Hext PM, Warheit DB, et al. 2004. Pulmonary responses of mice, rats, and hamsters to subchronic inhalation of ultrafine titanium dioxide particles. *Toxicol Sci* 77:347–57.
- Blum JL, Xiong JQ, Hoffman C, Zelikoff JT. 2012. Cadmium associated with inhaled cadmium oxide nanoparticles impacts fetal and neonatal development and growth. *Toxicol Sci* 126:478–86.
- Bolea E, Jimenez-Lamana J, Laborda F, Abad-Alvaro I, Blade C, Arola L, et al. 2014. Detection and characterization of silver nanoparticles and dissolved species of silver in culture medium and cells by AsFIFFF-UV-Vis-ICPMS: application to nanotoxicity tests. *Analyst* 139:914–22.
- Campagnolo L, Massimiani M, Palmieri G, Bernardini R, Sacchetti C, Bergamaschi A, et al. 2013. Biodistribution and toxicity of pegylated single wall carbon nanotubes in pregnant mice. *Part Fibre Toxicol* 10:21.
- Chen Z, Myers R, Wei T, Bind E, Kassim P, Wang G, et al. 2014. Placental transfer and concentrations of cadmium, mercury, lead, and selenium in mothers, newborns, and young children. *J Expo Sci Environ Epidemiol* 24:537–44.
- Davenport LL, Hsieh H, Eppert BL, Carreira VS, Krishan M, Ingle T, et al. 2015. Systemic and behavioral effects of intranasal administration of silver nanoparticles. *Neurotoxicol Teratol* 51:68–76.
- Dencker L, et al. ed., 1983. *Reproductive and Developmental Toxicity of Metals*. New York, NJ, USA: Plenum Press.
- Engler-Chiurazzi EB, Stapleton PA, Stalnaker JJ, Ren X, Hu H, Nurkiewicz TR, et al. 2016. Simpkins, Impacts of prenatal nanomaterial exposure on male adult Sprague-Dawley rat behavior and cognition. *J Toxicol Environ Health A* 79:447–52.
- Girard S, Tremblay L, Lepage M, Sébire G. 2010. IL-1 receptor antagonist protects against placental and neurodevelopmental defects induced by maternal inflammation. *J Immunol* 184:3997–4005.
- Gosens I, Cassee FR, Zanella M, Manodori L, Brunelli A, Costa AL, et al. 2016. Organ burden and pulmonary toxicity of nano-sized copper (II) oxide particles after short-term inhalation exposure. *Nanotoxicology* 10:1084–95.
- Gray EP, Coleman J, Bednar AJ, Kennedy AJ, Ranville JF, Higgins CP. 2013. Extraction and Analysis of Silver and Gold Nanoparticles from Biological Tissues Using Single Particle Inductively Coupled Plasma Mass Spectrometry. *Environ Sci Technol* 47:14315–23.
- Hayat M.A., ed., 1981. *Fixation for Electron Microscopy*. New York, NJ, USA: Academic Press.
- Hougaard KS, Campagnolo L, Chavatte-Palmer P, Tarrade A, Rousseau-Ralliard D, Valentino S, et al. 2015. A perspective on

- the developmental toxicity of inhaled nanoparticles. *Reprod Toxicol* 56:118–40.
- Huang JP, Hsieh PC, Chen CY, Wang TY, Chen PC, Liu CC, et al. 2015. Nanoparticles can cross mouse placenta and induce trophoblast apoptosis. *Placenta* 36:1433–41.
- Iavicoli I, Fontana L, Nordberg G. 2016. The effects of nanoparticles on the renal system. *Crit Rev Toxicol* 46:490–560.
- Juling S, Bachler G, von Götz N, Lichtenstein D, Böhmert L, Niedzwiecka A, et al. 2016. *In vivo* distribution of nanosilver in the rat: The role of ions and de novo-formed secondary particles. *Food Chem Toxicol* 97:327–35.
- Kreyling WG. 1990. Interspecies comparison of lung clearance of “insoluble” particles. *J. Aerosol Med* 3:S93–S110.
- Lebedová J, Bláhová L, Večeřa Z, Mikuška P, Dočekal B, Buchtová M, et al. 2016. Impact of acute and chronic inhalation exposure to CdO nanoparticles on mice. *Environ Sci Pollut Res Int* 23:24047–60.
- Miller FJ, Asgharian B, Schroeter JD, Price O. 2016. Improvements and additions to Multiple Path Particle Dosimetry model. *J Aerosol Sci* 99:14–26.
- Muoth C, Aengenheister L, Kucki M, Wick P, Buerki-Thurnherr T. 2016. Nanoparticle transport across the placental barrier: pushing the field forward!. *Nanomedicine (Lond)* 11:941–57.
- Myllynen PK, Loughran MJ, Howard CV, Sormunen R, Walsh AA, Vähäkangas KH. 2008. Kinetics of gold nanoparticles in the human placenta. *Reprod Toxicol* 26:130–7.
- Paris JJ, Brunton PJ, Russell JA, Frye CA. 2011. Immune stress in late pregnant rats decreases length of gestation and fecundity, and alters later cognitive and affective behaviour of surviving pre-adolescent offspring. *Stress* 14:652–64.
- Pietroiusti A, Massimiani M, Fenoglio I, Colonna M, Valentini F, Palleschi G, et al. 2011. Low doses of pristine and oxidized single-wall carbon nanotubes affect mammalian embryonic development. *ACS Nano* 5:4624–33.
- Prouillac C, Lecoœur S. 2010. The role of the placenta in fetal exposure to xenobiotics: importance of membrane transporters and human models for transfer studies. *Drug Metab Dispos* 38:1623–35.
- SCENIHR (Scientific Committee on Emerging and Newly Identified Health Risks), Nanosilver: safety, health and environmental effects and role in antimicrobial resistance, Date of adoption 10–11 June 2014.
- Scimeca M, Giannini E, Antonacci C, Pistolese CA, Spagnoli LG, Bonanno E. 2014. Microcalcifications in breast cancer: an active phenomenon mediated by epithelial cells with mesenchymal characteristics. *BMC Cancer* 14:286.
- Scimeca M, Pietroiusti A, Milano F, Anemona L, Orlandi A, Marsella LT, et al. 2016. Elemental analysis of histological specimens: a method to unmask nano asbestos fibers. *Eur J Histochem* 60:2573.
- Semmler-Behnke M, Seitz J, Erbe F, Mayer P, Heyder J, Oberdorster G, et al. 2004. Long-term clearance kinetics of inhaled ultrafine insoluble iridium particles from the rat lung, including transient translocation into secondary organs. *Inhal Toxicol* 16:453–9.
- Semmler-Behnke M, Takenaka S, Fertsch S, Wenk A, Seitz J, Mayer P, et al. 2007. Efficient elimination of inhaled nanoparticles from the alveolar region: evidence for interstitial uptake and subsequent reentrainment onto airways epithelium. *Environ Health Perspect* 115:728–33.
- Silver Nanotechnology Working Group, 2012. Comments on the NIOSH Request for information on Worker Exposure to Nanosilver. Available from: https://www.silverinstitute.org/site/wp-content/uploads/2013/05/SNWG_SKMBT2013.pdf. Accessed on 12 December 2012.
- Smulders S, Luyts K, Brabants G, Landuyt KV, Kirschhock C, Smolders E, et al. 2014. Toxicity of nanoparticles embedded in paints compared with pristine nanoparticles in mice. *Toxicol Sci* 141:132–40.
- Stone V, Miller MR, Clift MJ, Elder A, Mills NL, Møller P, et al. 2016. Nanomaterials vs Ambient Ultrafine Particles: an Opportunity to Exchange Toxicology Knowledge. *Environ Health Perspect*. Epub ahead of print. doi:10.1289/EHP424
- Sung JH, Ji JH, Park JD, Yoon JU, Kim DS, Jeon KS, et al. 2009. Subchronic inhalation toxicity of silver nanoparticles. *Toxicol Sci* 108:452–61.
- Thompson J, Bannigan J. 2008. Cadmium: toxic effects on the reproductive system and the embryo. *Reprod Toxicol* 25:304–15.
- Vance ME, Kuiken T, Vejerano EP, McGinnis SP, Jr Hochella MF, Rejeski D, et al. 2015. Nanotechnology in the real world: Redeveloping the nanomaterial consumer products inventory. *Beilstein J Nanotechnol* 6:1769–80.
- Wick P, Malek A, Manser P, Meili D, Maeder-Althaus X, Diener L, et al. 2010. Barrier capacity of human placenta for nanosized materials. *Environ Health Perspect* 118:432–6.
- Yamashita K, Yoshioka Y, Higashisaka K, Mimura K, Morishita Y, Nozaki M, et al. 2011. Silica and titanium dioxide nanoparticles cause pregnancy complications in mice. *Nature Nanotech Nanotechnol* 6:321–8.
- Yang H, Sun C, Fan Z, Tian X, Yan L, Du L, et al. 2012. Effects of gestational age and surface modification on materno-fetal transfer of nanoparticles in murine pregnancy. *Sci Rep* 2:847.